

BME SENIOR CAPSTONE PROJECT

PROJECT TITLE: Characterization of Brain Metabolic State under Injury using Two-Photon Microscopy

TEAM MEMBERS: Arrietty Bui, Kerry Chen, Varshini Ramanathan, Ash Sze

PRINCIPAL INVESTIGATOR: Irene Georgakoudi

ABSTRACT: Traumatic brain injury (TBI) is a leading cause of death and disability worldwide. However, TBI remains difficult to identify and treat in the clinic due to a lack of known biomarkers that can be used as diagnostic and therapeutic targets. To this end, 3D-engineered brain tissues seeded with human-induced neuronal stem cells (hINSCs) are assessed using multimodal label-free two-photon excited fluorescence (TPEF). TPEF generates endogenous fluorescence from several metabolic co-enzymes and stress-associated cellular products, which are measured by spectral intensity and fluorescence lifetime imaging. We aim to correlate optical measurements with biochemical and metabolomic assays in the context of two major aspects of TBI, glutamate excitotoxicity and oxidative stress. This work will ultimately be used to develop a metabolic model that will use optical measurements to identify biomarkers that are implicated in TBI-associated pathways.

KEYWORDS: Traumatic brain injury, two-photon imaging, metabolic pathways, mass spectrometry, 3D-engineered brain tissue, metabolic computational model

ELEMENTS OF ENGINEERING DESIGN:

The *design of this project* is the characterization of optical readouts by mapping them to specific metabolic pathways affected by injury. This can be achieved with a 3-compartment system: cell culture, imaging, and computational model. The *objectives* are based on each compartment. A specific injury will be induced in monoculture and 3D co-culture and its impact will be examined via microscopy, metabolic assays, and mass spectrometry. Computational models will be created to identify affected metabolic pathways from biochemical data. These *objectives can be tested and evaluated*. Once a comprehensive cell culture protocol has been developed, we will consider our cultures as viable if they remain stable at passage 3 and are healthy as observed in baseline imaging readouts, which will be compared to imaging readouts from validated cultures in the lab. Mass spectrometry will follow the validated protocols from the Lee lab. The acquisition of optical images will be adapted from the imaging protocols of the Georgakoudi lab. We will evaluate the successful induction of our injury conditions by asserting that trends of optical readouts and mass spectral data converge, indicating that the experimental treatment successfully induced a consistent metabolic shift. As an additional safety net, results from metabolic assays should agree with data from mass spec given both methods measure metabolomics concentrations.

Multiple *engineering principles* are applied in this project. First being two-photon microscopy (TPEF) - an imaging modality for injury assessment. Compared to standard fluorescence microscopy, TPEF utilizes a pulsed, non-linear excitation process where 2 photons are used to excite the fluorophore. By lowering the amount of energy needed per photon, TPEF uses a longer wavelength, which generates less tissue damage and penetrates deeper. Sufficient laser intensity for this excitation is only achievable in the focal plane. This restricts the volume of the signal generation as out-of-focus signals from the planes above and below the focal plane of the sample are removed. These characteristics make TPEF depth-resolved, facilitating the imaging of thick and highly scattering specimens like engineered brain tissue (EBT) without the need for slicing or biopsy. For this project, endogenous fluorophores such as FAD and NADH will be used so the imaging process is label-free where samples can be live imaged.

There are 2 *realistic constraints*: ethical concerns and translatability of the computational model. There are ethical concerns about incurring TBI in human brains or postmortem samples. As a *solution*, we will use 3D-engineered brain tissues which show pathophysiology observed in an *in-vivo* model [15]. While there are ethical concerns due to the use of human cells, this is necessary to accurately determine if our results are clinically translatable. Additionally, we plan to use a model of brain metabolism at baseline derived from literature because there is no complete TBI metabolic model. Metabolic model source code is difficult to obtain, and models may be designed based on assumptions and conditions specific to the institution which published that model. It may be a non-trivial task to adapt existing models to assist our project. A solution would be to write our own model based on the key differential equations governing the metabolic processes of interest to us (central metabolism, glutamate-glutamine conversion, and oxidative stress). This would be outside the scope of our capstone but would be doable by masters students.

DESIGN FLOWCHART

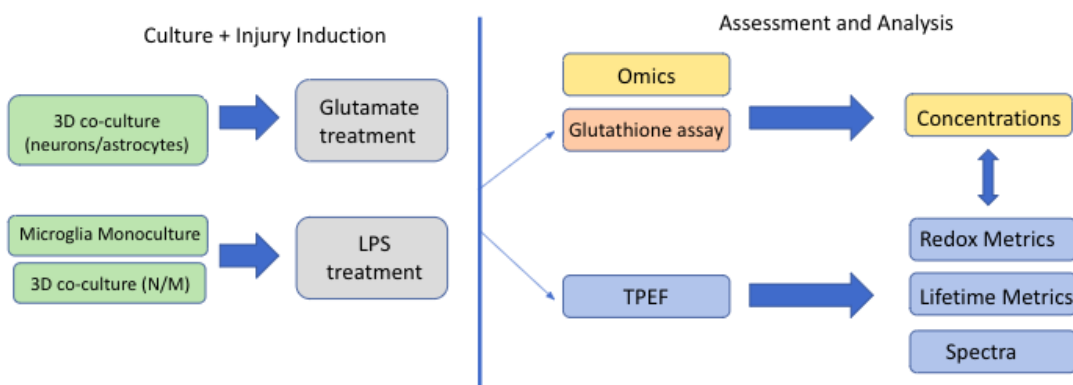


Figure 1.
Schematic
overview of
experimental
plan

DESIGN ELEMENT TABLE

Design Elements	Success Measures
LPS - microglia monoculture	Study 1: Optimize injury conditions Optical readouts indicate decrease in free NADH and glycolysis shift <ul style="list-style-type: none"> - Phasor shifts to bottom right - Redox ratio increases - Spectral constituents have an increased NADH concentration
LPS - 3D neuron-microglia co-culture Glutamate injury - neuron-astrocyte 3D co-culture	Study 1: Optimize culture conditions (NM scaffolds only) <ul style="list-style-type: none"> - No significant difference in optical readouts between Kaplan Lab's and our scaffolds Study 2: Optimize injury conditions (NM and NA scaffolds) Verify that, using statistical analysis, injury occurs <ol style="list-style-type: none"> a. Cell viability decreases after injury b. Glutathione assay indicates that glutathione is down-regulated in glutamate excitotoxicity c. Glutathione assay indicates an increased oxidized-reduced glutathione ratio for LPS condition (oxidative stress) Study 3: Induce and asses injury <ul style="list-style-type: none"> - The results of mass spectra and metabolic assays should be consistent with each other - Student's T-Test shows significantly different peak heights in glutamate and glutamine at 0h and 24h for glutamate excitotoxicity - The trend of optical readouts is similar to that of monoculture
Computational Model Differential Equations MATLAB Functions	<ol style="list-style-type: none"> 1. Investigate the outline and syntax required to create differential equations and their associated graphs 2. Establish a set of differential equations to model the concentration of upstream, TBI-related molecules using results from mass spec 3. Create functions using the differential equations on MATLAB to simulate specific concentrations at specific times <ol style="list-style-type: none"> a. Analyze the simulated upstream pattern for TBI indicators b. Verify the output of our function with experimental results

Table 1. Table describing design elements and success measures to validate and verify them.

INTRODUCTION AND BACKGROUND

Traumatic brain injury is the leading cause of death among individuals under the age of 45 in the US, with an incidence of 1.5 million each year. Beyond fatality, TBI results in severe long-term disabilities, both mentally and physically. [3] Traumatic brain injury can be divided into 2 phases: a primary mechanical impact on the brain followed by secondary biochemical and inflammatory cascades of different types of brain cells. The two major biochemical cascades that we plan to characterize are oxidative stress and glutamate excitotoxicity [9]. Following the injury, an influx of excess calcium ions into the mitochondria triggers the production of reactive oxygen species (ROS) and free radicals. These molecules depolarize the mitochondrial inner membrane, disrupting the electron transport chain and inhibiting the oxidative phosphorylation process. This deprives the nerve cells of ATP and facilitates apoptosis. In junction with oxidative stress, glutamate and aspartate neurotransmitters accumulate at the synapses as the impaired glutamate transporters fail to recycle excess glutamate from injured neurons. These molecules bind to NMDA and AMPA receptors that promote calcium, potassium, and sodium uptake. Cell depolarization triggers downstream cascades that prolong the effect of oxidative stress. From these observations, it can be said that the biochemical pathways involved in secondary injury are highly

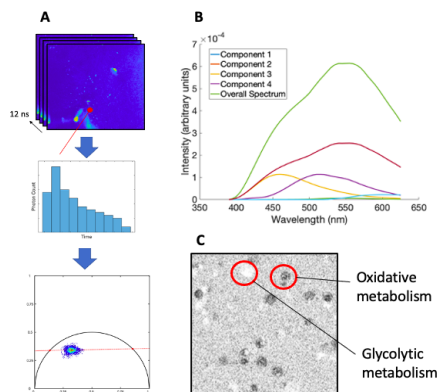
complex. Despite ongoing research, the understanding of its mechanisms and consequences remains incomplete. Secondary injury can develop to a greater severity over a long period of time. Patients with mild TBI can suffer neurological problems and long-term disability months after the injury. For this reason, patients with mild TBI have no initial symptoms and are often undiagnosed, preventing early treatment. The *long-term objective* is to develop a technique that can diagnose TBI on a molecular level, which is the biochemical cascade of secondary injury.

To examine the long-term cellular effects of mild TBI, the 3D-engineered brain tissues (EBT) of neurons and glial cells (astrocytes and microglia) are injured using the controlled cortical impactor (CCI), mimicking a mild blast TBI. The EBT model, while a simplified human brain, still undergoes most of the complex secondary response following the impact and, thus, can be used to develop diagnostic and treatment frameworks for TBI. However, with CCI, it is challenging to completely characterize this model due to the evolving complex cellular environment and unpredictable changes arising from the interactions between multiple cell types. Thus, we *propose* to examine TBI via its constituents by introducing a specific secondary injury to 2D brain cell cultures and studying the cellular metabolic interactions and environments in a controlled manner.

Two-photon excited fluorescence (TPEF) can then be used to assess functional and morphological changes of the injured brain cells by obtaining the metrics of cellular metabolic function. TPEF detects autofluorescent signals from several key biomolecules: FAD, NADH, LipDH, and lipofuscin. The former three are metabolic coenzymes implicated in most metabolic perturbations, and lipofuscin is a complex of fluorescent proteins and lipids that accumulates under cellular stress. These endogenous fluorophores can be analyzed using computational techniques that reveal concentration-based and metabolic shifts in the samples: redox ratio, mitochondrial clustering, phasor analysis, and spectral deconvolution.

The *redox ratio* is the relative ratio of glycolytic to oxidative metabolism. It is computed by obtaining a “NADH image” (755ex/460em) and a “FAD image” (860ex/525em) and dividing them according to the formula $(\text{NADH}/(\text{NADH}+\text{FAD}))$. *Mitochondrial clustering* is the extent of mitochondrial fractionation, which occurs in response to ROS accumulation. It is computed by segmenting and cloning mitochondrial regions in an image. Then, the power spectral density of the cloned image is computed, which determines the image frequency. Highly fractionated mitochondria will have a high frequency, and vice versa. *Phasor analysis* is a technique to obtain fit-free visualizations of FLIM images with overlapping concentrations of lifetimes over different pixels.

In brief, time-series fluorescence lifetime data is sine and cosine transformed, giving two coordinates g and s that correspond to the lifetime, τ , of the fluorescent decay. Any one τ localizes on a circular plot (see Fig. 2). The localization of the (g, s) coordinate pair for any given pixel is determined by the linear combination of different τ values constituent in the pixel. A fluorophore’s binding environment affects its lifetime, but its concentration does not (i.e. higher concentrations of a single fluorophore simply cause a shift in the phasor distribution towards that fluorophore’s lifetime). As such, by assessing the overall phasor distribution, conditions such as shifts in relative concentrations of



fluorophores and shifts in fluorophore binding configuration can be observed. *Spectral constituents* are obtained from the overall spectral intensity curve via non-negative matrix factorization. In this method of spectral deconvolution, the user specifies the number of total constituents and the model computes optimal concentrations of non-negative vectors and weights that minimize the error (residual) from the overall spectrum. In this way, concentrations and emission spectra of constituent fluorophores are determined.

Figure 2. Description of lifetime phasor analysis (a), redox ratio (b), and spectral deconvolution (c).

Compared to state-of-the-art diagnosis procedures like MRI, TPEF is more sensitive to cellular-level metabolic shifts. However, TPEF fails to detect non-fluorescence metabolites

such as lactate. While it is known that an increase in redox ratio correlates to an increase in glycolytic metabolism and vice versa, conducting redox ratio studies in conjunction with exact biochemical measurements will allow us to quantify how shifts in oxidative and glycolytic metabolism affect our optical readouts. This lack of specificity is a *critical roadblock* for using TPEF to study injured brain metabolism. Consequently, the *specific goal* is to characterize and map optical metrics to specific altered metabolic pathways predicted by a metabolic computational model. The *central hypothesis* for identifying the pathways is to input relevant biochemical metrics from assays and mass spectrometry to the computational model.

Two-photon imaging is a commonly used neuroimaging technique due to its high-depth penetration and potential for metabolic sensitivity. Many groups researching the impact of TBI or other neurodegenerative diseases choose to use two-photon imaging. Additionally, biological assay and mass spectrometric methods are well-investigated in the context of TBI [1-4]. Therefore, **the novelty of this project lies in correlating a non-invasive, label-free method (TPEF) with these invasive methods for the eventual use of optical methods alone for a diagnostic TBI model.** A non-invasive, label-free platform for the assessment of TBI does not exist to our knowledge. The novelty of this study depends on the identification of TBI biomarkers, not just the development of a two-photon platform to study TBI.

We propose to formulate a relationship between output molecular concentrations from assays and optical readouts via a computational model. We hypothesize that, under different perturbed or injured conditions, the trend in optical readouts and molecular concentration will be different since different metabolic mechanisms are involved. Therefore, we can say that a specific trend in optical readouts will be characteristic of a set of output concentrations and from the computational mode, specific altered metabolic pathways. This will allow us to characterize the optical readouts for a specific injury condition.

This work fits within research performed by Ph.D. candidate YangZhang and postdoctoral scholar Maria Savvidou in the ODDET Lab. They have acquired multimodal (spectral, fluorescence lifetime, and intensity) two-photon images of the EBT model under injury and control conditions. *Our work focuses on the specific characterization of aspects of TBI in simpler, controlled culture and injury settings in order to better understand correlation between cellular shifts and optical readouts in the EBT data.*

SPECIFIC AIMS, METHODS, AND RESULTS

Specific Aim 1 (SA1): Assessment of controlled secondary injury in monoculture

Injury to the 3D engineering brain tissue is induced in a non-specific manner via a stereotaxic impactor. In order to study a targeted metabolic cascade (secondary injury) of TBI such as glutamate excitotoxicity, specific metabolic perturbations must be introduced and changes to relevant metabolic pathways can be detected. Since this study has not been done previously, it's important that we perform a preliminary study on the monoculture to optimize treatment concentrations and refine detection methods.

Study 1: Induce secondary injuries to monoculture of microglia

Excess lipopolysaccharide (LPS) can be added to the microglia monoculture to trigger oxidative stress. LPS interacts with transmembrane signaling receptor toll-like receptor 4 which is expressed primarily on microglia. Our postdoc, Maria, has determined an optimal exposure time and concentration (1 ug/mL at 100 uL) which successfully induces LPS uptake in microglia. We will use 3 well replicates for each concentration at each time point, and one control set. To assess the cultures, we will use multimodal TPEF (see Data Acquisition) at 12 and 24 hours. At the last time point, mass spectrometry will be performed on the injured condition and the control condition.

The *success measure* is to validate that the optical readouts trend consistently toward glycolysis, as it is well-known that oxidative stress causes a shift to glycolytic metabolism. The phasor distribution should move to the bottom right to indicate increased free NADH, the redox ratio should increase, and spectral constituents should have an increased NADH concentration; all validations are based on previous ODDET lab work.

Data acquisition and analysis: The effect of the induced perturbations will be examined via TPEF. We will perform multimodal TPEF acquisition according to standard imaging protocols in the Georgakoudi

lab. Redox ratio, mitochondrial clustering, lifetime phasor distributions, and spectral constituents are obtained by custom-written MATLAB code.

Potential Pitfalls and Alternatives:

It is possible that we will encounter difficulties inducing sufficient glutamate uptake or dealing with unprecedented reactions to the addition and removal of exogenous glutamate. Alternatively, a previous study has shown that 200 μM of DL-TBOA is sufficient to inhibit the NMDA glutamate receptor and, thus, induce glutamate excitotoxicity without extraneous glutamate [14].

Specific Aim 2 (SA2): *Assessment of glutamate injury in neuron-astrocyte (NA) and LPS injury in neuron-microglia (NM) 3D co-cultures.*

Study 1: Optimize culture and injury (LPS and glutamate) conditions for 3D NA and NM

Cell culture: We will begin using NA scaffolds prepared by the Kaplan Lab's brain group, which are available to us through a collaborative project on neurodegeneration. As we conduct Study 2 onwards on these scaffolds, we will work on mastering the cell differentiation and seeding protocol so we can prepare our own scaffolds as per the Kaplan Lab's established protocol. For LPS injury, we will have to develop our own NM co-culture protocol in BME 8 ourselves, which may present difficulties and we may have to study only microglial monocultures. Our *success measure* will be a repetition of an imaging experiment under baseline conditions on both scaffolds seeded by the Kaplan Lab and us. Our *success measure* will be no significant difference in imaging readouts (TPEF redox ratio, FLIM phasor distributions, spectral emission) in our and the Kaplan lab's scaffolds.

Glutamate: We will test glutamate concentrations from 100-300 μM at exposure times of 15 and 30 minutes as well as a long exposure (6 hours), as per papers summarized in the Appendix. To achieve sufficient cell death caused by glutamate excitotoxicity, we will examine higher glutamate concentration. We will replace the cell media with a magnesium-free minimal medium for one day prior to injury because magnesium can occupy AMPA receptors and prevent glutamate activation. After glutamate exposure, we will rinse the scaffolds with minimal medium and replace them with the normal neurobasal medium.

LPS: We will test those conditions (100 $\mu\text{g}/\text{mL}$ at 100 μl , 24 hours exposure) as well as two auxiliary conditions (75 and 150 $\mu\text{g}/\text{mL}$) on the 3D scaffolds. We will image these cultures at 0, 6, 12, and 24 hours using two-photon spectral and FLIM imaging as described in SA 1. We will conduct 3 imaging replicates on one scaffold for three concentrations and time points, yielding 9 total datasets. We will *assess cell viability* visually, via manual image assessment, as dead cell bodies in scaffolds can be identified as round, bright debris in two-photon images. We will *assess success* by comparing imaging signal-to-noise ratio and cell death numbers to those acquired under optimal conditions in the previously-assessed 2D monoculture.

For success measure, we will *assess glutamate uptake* via a glutathione assay (Sigma Aldrich), as we expect glutathione to be down-regulated under glutamate excitotoxicity. We will *assess oxidative stress* as successful if we observe an increased oxidized-reduced glutathione ratio, as determined through the glutathione redox assay, as glutathione's antioxidant activity will be induced by the LPS activation.

Study 2: Induce glutamate and LPS injury and assess using imaging, mass spectrometry, and glutathione assay.

We will use our optimized conditions from Study 1 and induce glutamate excitotoxicity and LPS stress at one concentration and one exposure time with the media protocol described above. We will conduct a glutathione assay conducted at 12 and 24 hours and mass spectrometry conducted at 24 hours. We will image as described in SA1 for each injury condition.

Glutamate: We will use three imaging replicates on three injury scaffold replicates, with three imaging replicates on one control scaffold (medium change and rinse only) and one non-treated scaffold (no rinse and no glutamate). We will assess glutamate uptake as described in Study 2, and we will assess the effectiveness of the mass spectrometry protocol by observing significantly different peak heights in glutamate and glutamine at 0h and 24h (Student's T-Test).

LPS: We will use three imaging replicates on three injury scaffold replicates, with three imaging replicates on one control scaffold (LPS solvent medium only) and one non-treated scaffold. We expect to see a significant difference between *at least two* of the metabolite peak heights; unlike glutamate, we do not do the direct metabolic consequences of oxidative stress, so we cannot obtain a precise benchmark of success for the mass spectrometry peaks.

Data acquisition:

Imaging: As in SA 1.

Mass Spectrometry: Relevant metabolites (based on previous research) – glutamate, glutamine, creatinine, and decanoic acid – will be tagged so that their concentration changes can be detected with mass spectrometry [13]. The *goal* of using mass spectrometry in both studies is to identify metabolites that are heavily upregulated or downregulated after injury induction and verify that the detection method is suitable. To achieve this, we will conduct mass spectrometry at the start and end time points.

Data Analysis

Imaging: As in SA 1.

Mass Spectrometry: ANOVA with a post-hoc Student's t-test will be used to determine treatment concentration, for each study, that results in significant concentration change of desired metabolites.

Potential Pitfalls and Alternatives:

If no peaks are significantly different between baseline and injured mass spectrometry results, we will consider tagging different metabolites. We will have *verified* the LPS uptake by comparison with the previous benchmark, so we should not have to consider the lack of LPS uptake as a reason for failed results. However, we can perform Nile Blue staining of our scaffolds, which localizes to lysosomes and will stain the lipofuscin produced by oxidative stress, in order to ascertain that successful LPS uptake.

Specific Aim 3 (SA3): *Develop a computational metabolic model that predicts injury pathway activation based on biochemical readouts.*

Study 1: Develop a basic computational metabolic model for TBI cultures

We will obtain relevant brain metabolism computational models from the literature (neuron/astrocyte/microglia metabolism, oxidative stress models, and injury models) and modify them by adjusting concentration conditions based on our mass spectrometry results from SA 1 and 2. Molecules involved in the model but not present in our spectrometric results will be treated as assumed constants based on literature values. The completed model will include central metabolism, detoxification of reactive oxygen species, and the glutamate-glutamine cycle. It will be able to predict the relative level of pathway activation (ex. glycolytic vs. oxidative metabolism) based on the input concentrations of downstream metabolites obtained from mass spectrometry. We will validate the accuracy of our metabolic model by performing mass spectrometry on baseline cultures and assessing the similarity of our predicted pathway results with results obtained from the metabolic models from which our model was derived. This is to ensure that in integrating multiple models, we preserved the integrity of each individual model.

Study 2: Use the metabolic model to predict injury pathway activation

From SA 1 and 2, we will have imaging data from secondary injury at multiple time points and corresponding mass spectrometry data from the final time point. We can use the metabolite concentrations and the metabolic model to predict levels of pathway activation under injury conditions, and then correlate those pathway activations with the optical readouts from those same conditions. While the metabolic model does not output pathway activations, it predicts concentrations of upstream effectors that would cause observed downstream metabolite concentrations. By associating upstream effectors with particular injury pathways, we can estimate the pathway activations under different injury conditions.

There are a number of published models investigating brain metabolic injury pathways, including ODE-based modeling, flux balance analysis, metabolic diffusion analysis, multi-domain spatially distributed brain energy metabolism models, etc. Regarding microglia, a paper uses a flow

cytometry-based analysis using a controlled cortical impact model after TBI injury on mouse microglial cells, where isolated microglia undergo morphological changes and expression of activation markers are examined [16]. Another paper discussed using cytokine assays on microglial cells to see their regulatory mechanisms of microglia-mediated neuroinflammation. Specifically, a cytokine signaling network is established for the regulation of TNF α , IL-6, IL-10, TGF β , and CCL5 after introducing bacterial lipopolysaccharides (LPS) [17]. A 5-compartment model uses flux balance analysis to estimate the kinetic model parameters using the basis of glutamate concentration in the synaptic cleft and ATP hydrolysis. This model is governed by Michaelis-Menten equations on kinetic mass balance to see reaction rates and transport of the biomarkers [18].

Currently, there are no models that precisely cover our specific aims. However, the papers have a detailed outline of the differential equation sets that they used to derive their model, which we can replicate and modify. Our goal is to develop our own models for brain metabolite analysis using the existing models and mathematical equations.

Data Acquisition: This SA uses data obtained in SA 2.

Data Analysis: We will correlate optical readouts with pathway activations in LPS and glutamate conditions using a linear regression across time points. We will train on 4 out of the 5 replicates from SA 1 and test on the other using k-fold cross-validation. The regression will be validated based on a 0.85 Pearson correlation, and a statistically significant improvement for testing data from the wrong pathway to the correct pathway (i.e. glutamate optical readouts correlated against LPS concentrations should correlate significantly worse than glutamate readouts correlated against glutamate concentrations).

Potential Pitfalls and Alternatives: If the linear regression cannot separate the injury pathways, we will consider machine learning approaches. This will require much larger-scale data acquisition and would likely go beyond this project's scope. However, future students could improve replicates of this data across more concentrations. Then, they could use a logistic regression based on imaging and mass spectrometry raw data to directly classify imaging data as either glutamate-resultant or LPS-resultant.

PRELIMINARY RESULTS

We are using this space to describe the majority of our experimental progress. We do not directly address our Specific Aims in these experiments, but these experiments and analyses provide the foundation for which we will use to conduct our experiments and provide a baseline for our specific aims' results.

Cell culture Workflow

Arri and Kerry started cell culture training, specifically developing a cell passaging protocol, with HMC3 cell line with our postdoc Maria. Using this protocol, we will be able to work independently moving forward. We have established a cell line for our experiments that we are inducing injury on this/next week. *For the exact protocol, please see the Appendix.*

Imaging Workflow

We have spent time observing and practicing with our postdoc as she acquires imaging datasets from neuron-astrocyte (NA) scaffolds for a different project on HSV and Alzheimer's. The brain model is relevant but the outcome is not. We are being trained on this data to save time as Maria has 10-day acquisition periods which prevent her from being able work on the TBI project. Arri and Varshini have compiled an imaging protocol from this observation which will be used for our NA scaffold imaging for glutamate excitotoxicity. *For the exact protocol, please see the Appendix.*

LPS Microglial Optimization

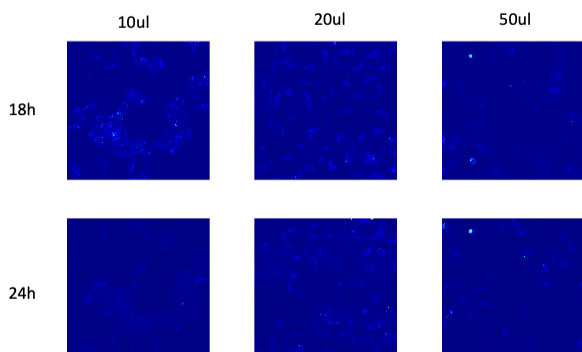


Figure 3. Optimization parameters for LPS induction in microglial monocultures. 2D plated microglia were incubated in varying concentrations of lipopolysaccharide (LPS) dissolved in DMSO and imaged after 18 and 24h.

Intensity is autofluorescent; separate staining using Nile Blue and DAPI was used to confirm that the observed structures are LPS-associated fluorescence (data not shown).

Images of increasing concentrations of LPS in microglia at 755 nm excitation and summed spectral emission (490-630 nm) are shown in Figure 3. The same regions were imaged at 18 and 24 hours post-induction. Images are normalized to maximum intensity. LPS localization, indicated by the saturated bright spots, is present at all concentrations and time points but is most noticeable at 50 μ M at 18h, and at 20 and 50 μ M at 24h. The same regions, particularly at 50 μ M, accumulate more LPS as a function of time. Additionally, at high concentrations, particular regions seem to preferentially uptake LPS, which is undesirable for studies of multiple cell regions. However, due to a lack of replicates – this pilot was done at 6 concentrations (3 concentrations are not shown) for 2 timepoints with only 1 sample per condition – no conclusions can be made about optimal concentrations, and optical readouts cannot be analyzed with statistical significance.

FLIM Phasor Preliminary Analysis

As the experimental process proceeds, Varshini has been working on FLIM analysis of primary mechanical injury and is trying to simulate the role of different fluorophores in causing a phasor distribution. The **goal of this analysis** is to develop an understanding of how *simultaneous activation of multiple injury pathways via primary injury affects FLIM readouts*, which will help us understand if pathway-specific injury can be determined via imaging readouts. We want to correlate the bulk metabolic shifts, upon primary impact, with the activation of particular secondary injury pathways. Therefore, it is important to understand what shifts the primary injury may be describing so that we have a framework upon which we can base our interpretation of the secondary injury studies that we describe in our Specific Aims. Framework findings are summarized below.

Varshini did a comprehensive analysis of phasor distributions from neurons, astrocytes, and microglia cultured on 3D scaffolds and subject to primary impact: controlled cortical impact, or CCI. They were imaged at 8h, 24h, and 48h. Here shows the major phasor distribution phenotypes present in the 8h data. 24h and 48h data are complicated by signal issues due to cell death and system issues.

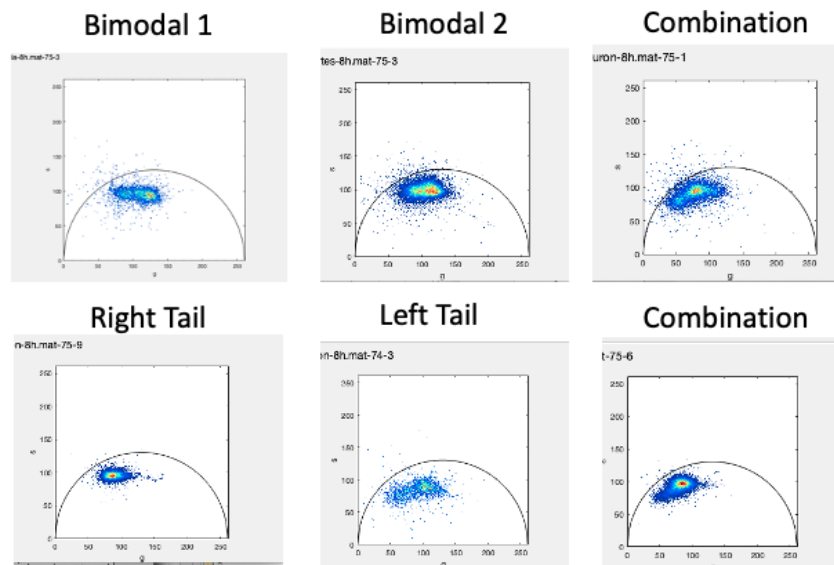


Figure 2. Characterization of Phasor Distributions in 8h Post-CCI Monocultures. Representative images of different phasor distribution phenotypes observed from neuronal, astrocytic, and microglial 3D monocultures imaged 8 hours post primary impact (CCI). Two distributions with combinations of multiple distribution types are also shown. The phenotypes are named descriptively/qualitatively as it remains unknown what the precise fluorophore contributions or underlying mechanisms are that determine each phenotype.

Modality of a phasor distribution determines how many distinct cellular populations there are in an image. A specific combination of fluorophores will localize as an elliptical, unimodal distribution (see Background figure). Non-injured phasors tend to be largely unimodal except for the occasional presence of the right tail. I suspect that the multi-modality of these distributions is a result of the metabolic response of certain cell types to injury. We do not know what fluorophore concentrations could be contributing to these separate distributions.

To this end, I used the **phasor distribution simulation** I developed last summer to test some possibilities of what fluorophores could be causing these multi-modal phenotypes. For now, I focused on the “Bimodal 1” phenotypes, which have a slight negative slope to the distribution with two distinct distributions localized on the left of the phasor distribution. I tested two possibilities, an increase in phosphate-bound NADH and an increase in FAD, which are shown in Figure 3.

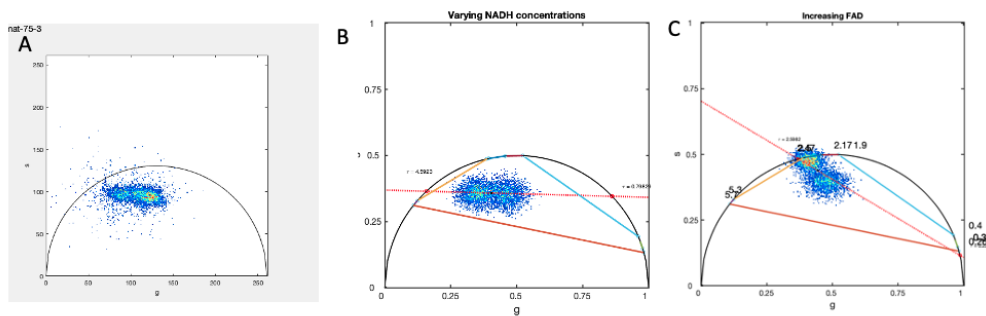


Figure 3. Simulation of 8h Post-CCI Phasor Distributions (a) An experimental distribution from 8h neurons which follows the “bimodal 1” phenotype. (b) Simulation of increasing bound NADH (NAD(P)H) in one half of the image, all other factors constant. (c) Simulation of increasing FAD in one half of the image, all other factors constant.

The bound NADH simulation correctly recapitulated the overall distribution location, but did not capture the negative slope of the distribution (compare the slope of the red line in (b) to the tilt of the distribution in (a)). To mitigate this, I tried simulating an FAD increase, which made the slope negative at an overshoot even with very minute concentration variations (0.1 difference between the two halves of the image). I suspect that the “bimodal 1” phenotype may be a combination of increased bound NADH and increased FAD.

These findings indicate that multiple fluorophore shifts associated with different metabolic processes are simultaneously activated under injury. Bound NADH and increased FAD are both associated with increased oxidative phosphorylation, which is consistent with the glycolytic depression that is known to occur in primary injury. However, the fact that cells are responding in distinct populations indicates a differential response to injury which could be **explained by the separate study of different secondary injury pathways**. From doing this analysis, I have learned that it will be important to assess the **phasor distribution multi-modality** and compare the population separations to those observed in the primary data to see if particular secondary injury pathways are responsible for particular cellular distributions. This is important foundational knowledge to understanding the fluorophore composition and cellular population separation in our primary injury data so that we can compare it to the data we plan to acquire of secondary injury.

Computational model framework and progress

The computational model will be built in MATLAB and relies on the differential equations provided by papers modeling metabolic pathways relevant to TBI. Blood flow equations will not be used because it does not apply to our engineered tissue models. Our goal is to create a system of first order differential equations which takes experimental results from our project and outputs downstream values. Certain constants and inputs will need to be inferred from papers or just be set to a constant value.

Varshini used ordinary differential equations (ODEs) in MATLAB for her systems biology class. Using that prior knowledge, she instructed Ash on the basics of the process. He investigated Varshini's existing code along with the equations provided by the metabolic modeling papers. In order to implement an ordinary differential equation, we first need to set rate parameters which cannot be modified. These will be values provided by the papers we read. Second, we need to set initial concentrations which would depend on experimental results. The ODE implementation puts the variables together such that they can be solved by an ODE and plotted using multiple conditions. The example below uses $S_0 = 0.07$ and $E_0 = 1.0$ but the values can be changed or written as vectors to model multiple conditions. The example ODE below is not specific to any metabolic pathway. It is a test run using ode23s in order to better understand how to implement more complicated equations in the future.

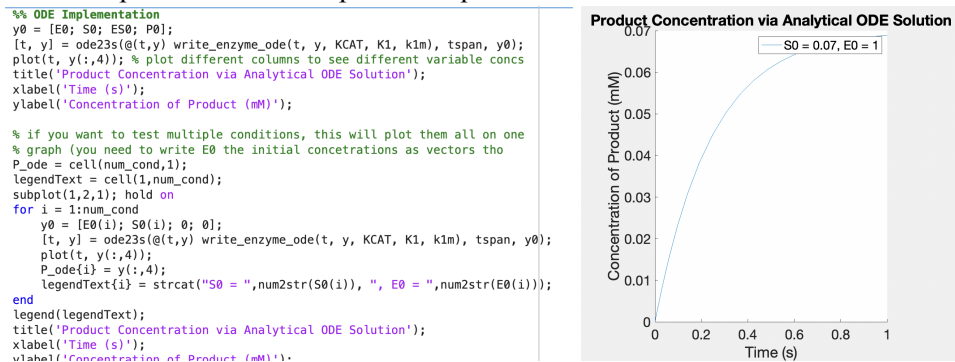


Figure 4. ODE implementation on MATLAB for a sample graph of product concentration over time via an Analytical ODE solution

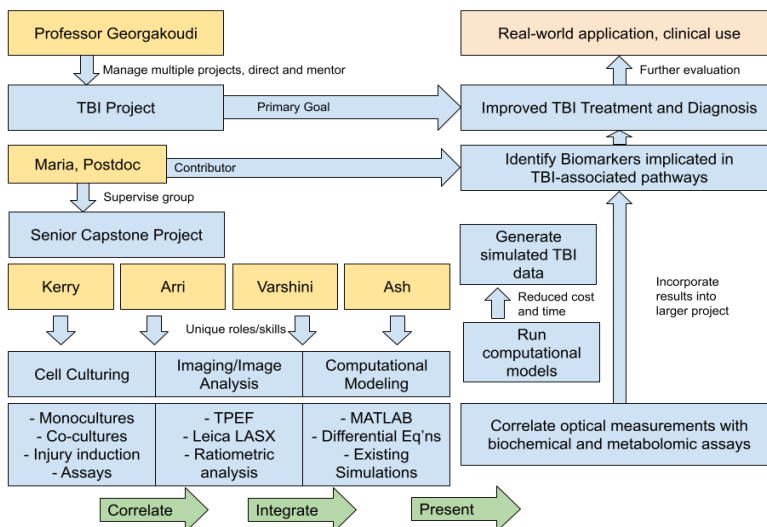
DISCUSSION AND FUTURE WORK

In the first semester, we read through papers relevant to TBI metabolism and TPEF imaging. We communicated with our post-doc and lab professor to start training for culturing microglia and using them for TPEF imaging. We developed a protocol for inducing and assessing secondary injury in co-culture models completely from scratch, which took significant efforts to rework and optimize given constraints of the Georgakoudi lab in cell culture methods. We researched the computational model using papers which aimed to do the same using differential equations. We have prepared our cell culture and imaging to induce our first injury experiment next week. In the second semester, we hope to finish developing our mono- and co-cultures for imaging and metabolic analysis, and have a framework for the metabolic model. With monoculture data from the first semester, we will be able to link the optical readouts with the metabolic data using statistical tools on MATLAB. We can compare this correlation in data to our computational model framework and adjust it as needed.

The goal of our project is to correlate optical measurements with biochemical and metabolomic assays. Understanding this correlation will allow us to develop algorithms to predict biochemical and metabolomic data purely from optical readouts. This is valuable because it reduces the time and cost required to see the metabolic effects of TBI on brain cells. Culturing cells and completing assays can cost thousands of dollars over the span of many months. The development of this algorithm will make it possible to do TBI research in a shorter time span and a smaller budget. This broadens the availability of TBI research to labs that do not have the resources to do cell culturing long-term. This also helps address the morality of using engineered brain tissue because it reduces the need for handling it.

UNIFYING FIGURE

BME7: Characterization of Brain Metabolic State under Injury using Two-Photon Microscopy (F'22)



Supp. Figure 1. The unifying figure describes a hierarchy of the lab, roles and objectives of our project, contribution of our project to the main project, and real world implications.

INDIVIDUAL CONTRIBUTIONS

Computational modeling includes compiling code on brain metabolic pathways affected by TBI, extracting valuable functions from external sources and writing code in MATLAB to analyze patterns in data found through co-cultures and imaging. Imaging includes using multi-modal two-photon microscopy to observe engineered brain cell activity after simulated concussions. Imaging will be done on monocultures first, then co-cultures in the second semester if there is enough time. Image analysis includes ratiometric analysis of different detector channels, phasor analysis, data processing, cellular segmentation and automatic annotation. This data will be correlated with cell culturing data. Cell culturing includes developing co-cultures and writing the secondary injury protocol. We are starting by culturing microglia because there exists an established protocol. The goal is to culture neurons and co-cultures, and collect metabolic data for correlation to image analysis results.

Ash will be responsible for computational modeling and assisting with image analysis under guidance from Varshini as she has experience from systems biology. The first task in computational modeling is to compile existing code that models glutamate excitotoxicity, lipofuscin, general brain metabolics and any other pathways relevant post TBI. These models will likely be used on MATLAB in the form of differential equations. Ideally, the models can successfully model chemical outputs given optical readouts.

Varshini will be responsible for guiding team members through higher-level computational work and imaging/image analysis. Varshini will be the main point of contact with the post-doc, Maria, who will further instruct Kerry and Arri in how to culture engineered brain tissue cells. She will be able to connect relevant resources from the Georgakoudi lab to our project such as existing protocols and models. Varshini has also been instructing Ash on using ODEs for MATLAB and imaging for all project members.

Kerry will be responsible for imaging and cell culturing. She will be familiarizing herself with TPEF and using her experience in cell culturing to guide Arrietty. Kerry will be receiving Microglia cell culturing instruction alongside Arri by post-doc Maria. She used available protocols and online papers to include well numbers, replicates, time points, duration of chemical exposure, correlating measurements and

number of trials into the draft protocol. Kerry has compiled many computational modeling papers, many of which contain useful ODEs for the model.

Arrietty will be responsible for developing co-cultures and writing the secondary injury protocol. She will also be using her experience to help with image analysis. Arri has been using her existing knowledge of computational modeling to find models for TBI chemical pathways. Working closely with Varshini, Arri is also communicating with Maria and the professor about possible alternatives for our project and training. She has also been further assisting with finding computational models that are relevant to the pathways we are studying.

All members of the project have completed the initial training required to work in the lab. We were able to catch up with our schedule. We have been able to define challenges, alternatives and specifics (timestamps, replicates, etc.). Currently, we are focusing on hands-on training and establishing the framework for our computational model.

REFERENCES

1. Haenseler, W. *et al.* A Highly Efficient Human Pluripotent Stem Cell Microglia Model Displays a Neuronal-Co-culture-Specific Expression Profile and Inflammatory Response. *Stem Cell Reports* **8**, 1727–1742 (2017).
2. Chapman, G. A. *et al.* Fractalkine Cleavage from Neuronal Membranes Represents an Acute Event in the Inflammatory Response to Excitotoxic Brain Damage. *J. Neurosci.* **20**, RC87–RC87 (2000).
3. Dorsett, C. R. *et al.* Glutamate Neurotransmission in Rodent Models of Traumatic Brain Injury. *J Neurotrauma* **34**, 263–272 (2017).
4. Wu, Y.-H. *et al.* In Vitro Models of Traumatic Brain Injury: A Systematic Review. *Journal of Neurotrauma* **38**, 2336–2372 (2021).
5. Robertson, J. M. Astrocyte domains and the three-dimensional and seamless expression of consciousness and explicit memories. *Medical Hypotheses* **81**, 1017–1024 (2013).
6. Bylicky, M. A., Mueller, G. P. & Day, R. M. Mechanisms of Endogenous Neuroprotective Effects of Astrocytes in Brain Injury. *Oxidative Medicine and Cellular Longevity* **2018**, 6501031 (2018).
7. Kim, O. D., Rocha, M. & Maia, P. A Review of Dynamic Modeling Approaches and Their Application in Computational Strain Optimization for Metabolic Engineering. *Frontiers in Microbiology* **9**, (2018).
8. Oschmann, F., Berry, H., Obermayer, K. & Lenk, K. From in silico astrocyte cell models to neuron-astrocyte network models: A review. *Brain Research Bulletin* **136**, 76–84 (2018).
9. Ng, S. Y. and A. Y. W. Lee. "Traumatic Brain Injuries: Pathophysiology and Potential Therapeutic Targets." *Front Cell Neurosci* **13**: 528, (2019).
10. Shi, H., *et al.* "The in vitro effect of lipopolysaccharide on proliferation, inflammatory factors and antioxidant enzyme activity in bovine mammary epithelial cells." *Anim Nutr* **2**(2): 99-104, (2016).
11. Mark, L. P., *et al.* "Pictorial review of glutamate excitotoxicity: fundamental concepts for neuroimaging." *AJNR Am J Neuroradiol* **22**(10): 1813-1824, (2001).
12. Chapman, G. A., *et al.* "Fractalkine cleavage from neuronal membranes represents an acute event in the inflammatory response to excitotoxic brain damage." *J Neurosci* **20**(15): RC87, (2000).
13. Posti JP, Dickens AM, Orešič M, Hyötyläinen T, Tenovuo O. Metabolomics Profiling As a Diagnostic Tool in Severe Traumatic Brain Injury. *Front Neurol*. doi: 10.3389/fneur.2017.00398. (2017)
14. Gupta, K., *et al.* "NMDA receptor-dependent glutamate excitotoxicity in human embryonic stem cell-derived neurons." *Neurosci Lett* **543**: 95-100. (2013).
15. Liaudanskaya, Volha *et al.* "Modeling Controlled Cortical Impact Injury in 3D Brain-Like Tissue Cultures." *Advanced healthcare materials* vol. 9,12 (2020).
16. Toledano Furman, N., Gottlieb, A., Prabhakara, K.S. *et al.* "High-resolution and differential analysis of rat microglial markers in traumatic brain injury: conventional flow cytometric and bioinformatics analysis." *Sci Rep* **10**, 11991 (2020).
17. Anderson, W. D. *et al.* "Computational modeling of cytokine signaling in microglia." *Royal Society of Chemistry* **12**. (2015).
18. Calvetti, D. *et al.* "Dynamic activation model for a glutamatergic neurovascular unit". *Journal of Theoretical Biology*, Volume 274, Issue 1, 12-29 (2011).

APPENDIX

1. Transwell 2D co-cultures are not compatible for confocal/two-photon imaging:
 - a. <https://www.corning.com/catalog/cls/documents/application-notes/CLS-AN-521-A4.pdf>
 - b. https://www.researchgate.net/post/Can_transwell-cultured_Caco-2_monolayers_be_imaged_with_BD_Pathway_confocal_microscopy_while_keeping_them_in_transwell
2. Glutamate Protocol Table

Arri has reviewed the relevant papers to identify different media compositions that were used. Using this information, we are working on refining the protocol for the glutamate excitotoxicity study. Additionally, given that most of the paper that we found were using 2D cultures, we plan to look at other papers that use 3D cultures to determine if a change of medium is required prior to the injury induction. The upper range of the glutamate concentration we use (300uM) is higher than that mentioned in the papers because, unlike the paper, we will use 3D culture, and 3D diffusion is worse than 2D diffusion.

Ref	Relevance	Glutamate Concentration	Exposure	Media/rinse	Notes
https://www.sciencedirect.com/science/article/pii/S0304394013002152	HESCs treated with glutamate at physiological concentrations	200 uM	24h	DMEM (with supplements) first and then changed to Neurobasal-A (with supplements) 50uM DAPT was included in first medium change	Changed to trophically deprived, glutamate-free minimal medium (90% salt-glucose-glycine medium and 10% MEM) 1 day prior to injury
https://www.ncbi.nlm.nih.gov/pmc/articles/PMC6773069/	NMDA and glutamate on rat cortical culture	100 and 300 uM	30 minutes	Control media = MEM + 0.01% BSA + 25mM HEPES + 10 um glycine Rinse: MEM 200:1 dilution	Younger culture is less sensitive so use higher conc. No change of medium prior to experiment After toxicity assay: cells are exposed to control solution, NMDA, or glutamate for 30 mins and then rinse
https://www.nature.com/articles/cddis2012194	rat derived hippocampal, cortical, midbrain neurons	100 uM glutamate 10 uM glycine, Mg ²⁺ free medium	15 minutes	HBSS (hippocampi) Neurobasal medium (Gibco-Invitrogen) supplemented with B-27 (Gibco-Invitrogen) and 2 mM L-glutamine (culture)	No change of medium prior to experiment

https://onlinelibrary.wiley.com/doi/full/10.1046/j.1471-4159.2000.0751045.x	mouse cortical cultures	100 to 500 uM	Didn't remove, glutamate media because they were testing enzyme degradation	Medium: Neurobasal medium, 2% B27, 0.5 mM L-alanyl-L-glutamine, 100 U/ml penicillin, 100 µg/ml streptomycin, 0.25 µg/ml amphotericin (Life Technologies) + 1% horse serum	No change of medium prior to experiment
https://www.nature.com/articles/s41419-018-0351-1	Rat hippocampal neurons from Wistar rat E18 embryos	30 and 100 uM (100 is most sig) Also test at 1 and 10 uM but not sig	30 mins	For low-astrocyte cultures: cytosine with AraC (Sigma-Aldrich) at conc. of 2 uM at DIV2-5	No change of medium prior to experiment
https://journals.biologists.com/jcs/article/131/22/jcs214684/56996/Axonal-degeneration-induced-by-glutamate	(E18 Sprague-Dawley) Rat embryonic hippocampal neurons	20uM	6 hours	After 3 h, the plating media was changed to Neurobasal™ medium supplemented with 2% B27, 0.5 mM GlutaMAX™-I and P/S After 3 days, a third of medium was replaced and treated with 5 uM AraC to inhibit glial cell proliferation	No change of medium prior to experiment

Table 2. Glutamate concentration, media composition, and injury exposure time for glutamate excitotoxicity induction of different cell lines from published literature.

Useful equations	Parameters	Application
$S \times v = 0$ $v_{min} \leq v \leq v_{max}$ $\min f^T v$ $\min \sum_i v^2 i$ $f^T v = objfun$	<p>S: m by n stoichiometric matrix</p> <p>m: # metabolites</p> <p>n: # reactions (covers pathway and exchange reactions)</p> <p>v: flux vector</p> <p>v_{min} and v_{max}: bounds of fluxes based on reversibility information</p> <p>f: row vector. Set to 0 except entries corresponding to fluxes that need to be maximized</p> <p>$objfun$: optimal value of objective function obtained in linear optimization of $\min f^T v$</p>	<p>Flux analysis of coupling between astrocytes and neurons. Flux-based analysis is a solution technique of systems using linear or quadratic programming to obtain an optimum solution. Used to identify metabolic flux distributions in and between astrocytes and neurons.</p> <p>Optimization through minimization of Euclidean norm to ensure channeling all fluxes through all pathways. For objective function, select the flux distribution with the minimal sum among all optima.</p>
$v_b \frac{d[A]}{dt} = \frac{Q}{F} ([A]_{arterial} - [A]) - J_{A,b \rightarrow ECS} + J_{A,ECS \rightarrow b}$	<p>$Q = Q(t)$: blood flow</p> <p>$[A]_{arterial}$: arterial concentration of species A</p> <p>F: mixing ratio to make sure $[A]$ is well-mixed. $0 < F < 1$.</p> <p>$J_{A,b \rightarrow ECS}$ and $J_{A,ECS \rightarrow b}$: account for transport fluxes of species A from blood to ECS and from ECS to blood.</p>	<p>Convection and transport across blood brain barrier regulate species concentrations in capillary compartment.</p> <p>Mass balance equation for $[A] = [A]_b$.</p>
$[O_2]_{tot} = [O_2]_{free} + 4Hct[Hb]_{rbc} \frac{([O_2]_{free})^2}{K_H^n + ([O_2]_{free})^2}$	<p>H_{ct}: hematocrit</p> <p>$[Hb]_{rbc}$: concentration of hemoglobin in red blood cells.</p>	<p>Mass balance equation for total concentration of oxygen, which is the sum of free and bound oxygen.</p>
$J_{A,x \rightarrow y}(t) = \lambda([A]_x(t) - [A]_y(t))$		<p>Passive transport of species A from compartments x to y.</p>
$J_{A,x \rightarrow y}(t) = T_{max} \frac{[A]_x(t)}{M + [A]_x(t)}$	<p>T_{max}: maximum transport rate</p> <p>M: affinity constant</p>	<p>Facilitated transport (requires intervention of membrane bound transporter x)</p>

$J_{Glu,n \rightarrow c}(t) = T(t) \frac{[Glu](t)}{M(t) + [Glu]_n(t)}$	<p>$J_{Glu,n \rightarrow c}$: transport rate of glutamate from neurons to synaptic cleft</p> $T(t) = T_0(1 + 2u(t))$ $M(t) = M_0(1 - \frac{u(t)}{2})$ <p>T_0, M_0: low activity</p>	<p>Assumption: maximum transport rate and affinity increase with activity. This equation models glutamate exocytosis.</p>
$\Phi_{ATPase}(t) = \Phi_{base} + V_{max} f([Glu]_c) \frac{[ATP]_n}{K + [ATP]_n}$	<p>Sigmoidal saturation function of the form:</p> $f([Glu]_c) = \frac{[Glu]_c^2}{k_{Glu} + [Glu]_c^2}$	<p>ATP hydrolysis in neuron</p>
$\frac{dV_b}{dt} = \frac{1}{\tau} \left(\frac{Q(t)}{Q_{low}} - \left(\frac{V_b}{V_{b,low}} \right)^{1/\kappa} \right)$	<p>The semi-empirical values κ and τ (time constant) are set to 0.4 and 2 s, respectively.</p>	<p>This is the differential equation which the volume of blood compartment satisfies.</p>
$\frac{dm_A}{dt} = Q(t) \left([A]_{art} - \frac{m_A}{V_b(t)} \right) - J_{A,b \rightarrow ECS} + J_{A,ECS \rightarrow b}$	<p>A: substrate in blood compartment (Glc, Lac, O₂, CO₂). $m_A = [A]_b V_b$: mass of A.</p>	<p>Mass balance equations express the change in time of the metabolic masses, from which the concentrations can be calculated.</p>
$V \frac{d}{dt} \begin{bmatrix} C_b \\ C_{ECS} \\ C_c \\ C_n \\ C_a \end{bmatrix} = \begin{bmatrix} (Q/F)(C_{b,art} - C_b) \\ 0 \\ 0 \\ 0 \\ 0 \end{bmatrix} + \begin{bmatrix} 0 \\ 0 \\ 0 \\ S_n \Phi_n \\ S_a \Phi_a \end{bmatrix} + \begin{bmatrix} -J_{b \rightarrow ECS} + J_{ECS \rightarrow b} \\ J_{b \rightarrow ECS} - J_{ECS \rightarrow b} - J_{ECS \rightarrow n} - J_{ECS \rightarrow a} + J_{n \rightarrow ECS} + J_{a \rightarrow ECS} \\ J_{n \rightarrow c} - J_{c \rightarrow n} + J_{a \rightarrow c} - J_{c \rightarrow a} \\ -J_{n \rightarrow c} + J_{c \rightarrow n} - J_{n \rightarrow ECS} + J_{ECS \rightarrow n} \\ -J_{a \rightarrow c} + J_{c \rightarrow a} - J_{a \rightarrow ECS} + J_{ECS \rightarrow a} \end{bmatrix}$	<p>$C_b, C_{ECS}, C_c, C_n, C_a$: vectors of concentrations in blood, extracellular space, synaptic cleft, neuron, and astrocyte. $S_{a/n}$: stoichiometric matrices $\phi_{a/n}$: vectors of the reaction rates in astrocyte/neuron Diagonal entries of matrix V are volumes of the corresponding compartment</p>	<p>Analysis of steady states at low neuronal activity. At steady state, the system becomes: $V^{-1}(Au + r) = 0$ where $u = \begin{bmatrix} \Phi_n \\ \phi_a \\ J \end{bmatrix}, \quad r = \begin{bmatrix} (Q/F)(C_{art} - C_b) \\ 0 \\ 0 \\ 0 \\ 0 \end{bmatrix}$</p>

Table 3. List of differential equations involved in TBI which are relevant to our computational model and project.

Sources: (Çakir, 2007) and (Calvetti, 2010)

Protocol for passaging cell:

Materials needed: DMEM cell culture medium, trypsin, HMC3 cells in cell culture dish.

1. Warm the DMEM and trypsin in a 37°C water bath for 15~20 minutes.
2. Spray the biohood workspace w/ 10% bleach, 75% ethanol and wipe surface with tissue paper.
 - a. Applicable to any items brought into the hood
3. Aspirate old media from the cell culture dish
4. Wash twice with 5 mL PBS
 - a. Aspiration of the PBS should not be in contact with cells attached to the dish bottom
 - b. After adding PPBS, shake disk gently to distribute PBS

5. Add 1.5 mL of 0.25% trypsin-EDTA and put the dish in the 37°C incubator for 2-3 minutes
 - a. After 2-3 minutes, use microscope to check confluency / cell suspension
6. Add 8.5 mL of media to the cell culture dish
7. Transfer the cells (with trypsin and cell culture media) into a 15 mL conical centrifuge tube
8. Centrifuge at 1500 rpm for 3 minutes to pellet the cells
9. Aspirate cell culture media in conical centrifuge tube and re-suspend the cell pellet in 5 mL of new cell culture media
 - a. Gently pipette to mix and avoid bubbles
10. Calculate the desired seeding ratio and add the corresponding amount of cell suspension and media to the new cell culture dish
 - a. This depends on when the cells will be used
 - i. We plan to independently practice cell passaging in 5 days so we picked a ratio of 1:5 so that sufficient confluency is reached. This means that $\frac{1}{5}$ of the cell suspension (0.5mL) and 9.5 mL of new medium are needed for a 10 mL dish
 - ii. Extract 0.5 mL of the cell suspension from conical centrifuge tube and gently inject into the new cell culture dish with 9.5 mL of fresh media
 - b. Tilt the dish in north-west-south-east direction to distribute the cells
11. Aspirate and discard the old cell suspension in the centrifuge tube to biohazard bin
12. Put the new cell culture dish in the 37°C incubator overnight

The protocol reads as follows:

In general, we will measure spectral intensity at 755nm, 860 nm and 910nm excitation, detecting on a multi-wavelength PMT every 10 nm from 490 to 630 nm. We will measure fluorescence lifetime at the same excitations but detect only at 460 and 525 nm using a hybrid detector and a PicoQuant TCPSC module which allows for the high temporal resolution needed for fluorescence lifetime imaging.

1. Maintain Excel spreadsheet from centralized code base (on Georgakoudi network drive) to auto-generate file names for control and injury scaffolds.
2. Maintain plastic well plate with labeled control and injured scaffold sections and numbered wells to track each ROI throughout timepoints.
3. For each scaffold, remove from its place in the well and secure it with a metal harp to a glass bottom dish. Place the smooth (non-cut) side up.
4. Set the 40x water objective and add one drop of DI water. Lower the objective z stage fully and secure the dish in the sample stage.
5. Search for cells using brightfield eyepiece viewing. Cells are transparent in this mode but the edges can be seen when adjusting the Z height. Once cells are found, turn off the microscope internal light and lower all coverings, then confirm the presence of cells in Live imaging mode
6. Set the depth range based on the range of visible cells. Z slices are 4 microns apart.
7. Begin with intensity acquisition mode (xyz). All settings (line average, frame average) are set to 1, except for 8 frame accumulation. Speed is 60, bidirectional. The pinhole is at 1 AU (airy units).
8. Turn on the transmission PMT and both PMTs and HyDs.
9. Set and tune the wavelength for 755 nm.
10. Begin acquisition. Save name according to spreadsheet.
11. Repeat for 860, changing the depth by +1 micron to adjust for laser co-registration.
12. Change to FLIM acquisition mode. Set CFD (voltage) to 40 for 755, 60 for 860. Acquire and ensure that decay traces are smooth with no interruption. FLIM data is saved and renamed individually.
13. Change to spectral acquisition mode (xy-lambda). Change detector to the wavelength-adjusting PMT. Open the pinhole to 7.77 AU (full opening).
14. After spectral acquisition, change the pinhole back to 1 AU immediately to prevent photobleaching.
15. Repeat for as many ROIs are acquired per scaffold.

16. Retrieve the plastic well plate from the incubator. Return to the hood. Spray a tweezer with ethanol and dry in the hood. Pick up the scaffold from the edge and return to its original well. Retrieve the next scaffold and continue.